Available online at www.sciencedirect.com
SCIENCE DIRECT®
Journal of Nuclear Materials 345 (2005) 167–183
journal of nuclear materials
www.elsevier.com/locate/jnucmat

Selection of optimum microstructure for improved corrosion resistance in a Ti–5%Ta–1.8%Nb alloy

R. Mythili, S. Saroja, M. Vijayalakshmi *, V.S. Raghunathan

Materials Characterization Group, Indira Gandhi Centre for Atomic Research, Kalpakkam 603 102, India

Received 13 October 2004; accepted 3 May 2005

Abstract

This paper presents the results on (i) selection of microstructure with improved corrosion resistance in a Ti–5%Ta–1.8%Nb alloy and (ii) optimization of thermo-mechanical treatment to achieve the desirable structure. Ti–5%Ta–1.8%Nb is an $\alpha + \beta$ alloy and the decomposition of bcc $\beta \rightarrow \alpha + \beta$ is found to proceed via a number of transformation modes leading to different morphological products of α and β. The distribution of isolated β particles in a matrix of equiaxed α offered superior corrosion resistance in comparison to a lamellar $\alpha + \beta$ structure. In an attempt to obtain this desired structure, the β annealed alloy with a lamellar structure was subjected to a series of thermal and thermo-mechanical treatments. A combination of thermal and mechanical treatments was found to be essential to achieve the structure of equiaxed α with discrete β particles.

1. Introduction

Extensive research has been carried out to develop corrosion resistant materials for use in reprocessing plants of nuclear fuels [1]. These efforts have identified four different classes of alloys suitable for use in boiling nitric acid medium. These include low carbon 300 series Stainless Steel [2,3], high Cr, Ni-based RW alloys [4], Ti and Zr-based alloys [4,5]. While the former two series of alloys are well studied with respect to long-term industrial use, the latter two are being developed with limited data on industrial use. In case of SS and RW alloys, it is established that optimization of corrosion behavior can be achieved by (a) modification of the alloy chemistry, for example increase in Cr, Ni (maximum possible) and Si (0.1–0.2 wt%), (b) scavenging of impurity elements like P, S, B, N by purification procedures and (c) tailoring the microstructure. A similar comprehensive strategy for Ti and Zr-based alloys has not been developed so far. It is reported [4] that Ti-based alloys show excellent promise for future development.

However, at the laboratory scale, a number of Ti-based alloys with high corrosion resistance in boiling nitric acid medium [6] have been developed, based on certain broad design principles and guidelines. Corrosion properties of Ti alloys has been found to improve by alloying with elements possessing the following properties: (i) same metallic ion size as Ti, (ii) lowering the solubility of Ti in nitric acid and (iii) stabilization of the passive oxide film. Of the various elements studied, only Ta and Nb satisfy the above conditions [4,6]. The corrosion resistance of Ti alloys is reported [4] to improve in the ratio of 1:10:15 for Ti:Ti–5%Ta:Ti–5% Ta–1.8%Nb. Of these alloys Ti–5%Ta–1.8%Nb alloy has the minimum corrosion rate. The main limitation of this alloy is its

* Corresponding author. Tel.: +91 4114 280306; fax: +91 4114 280301.
E-mail address: mvl@igcar.ernet.in (M. Vijayalakshmi).

0022-3115/$ - see front matter © 2005 Elsevier B.V. All rights reserved.
doi:10.1016/j.jnucmat.2005.05.007

low corrosion resistance in the trickle zone, which is attributed to the 'desquamation' or destabilization of the oxide layer at the liquid–vapor interface [7].

Though the corrosion rate of Ti alloys is mainly altered by the chemical effect of alloying elements, secondary features like microstructure also impart significant influence [8]. The existing industrial experience with commercial grade Ti with iron content $\geqslant 0.05\%$ shows that failure of Ti equipment in nitric acid occurs due to preferential attack along the $\alpha - \beta$ lamellae in weld regions. It is also known that microstructure of the weld regions cannot be tailored by any thermo-mechanical processing. A similar effect has been observed in a number of Ti alloys used in corrosive media [8,9]. A microstructure of equiaxed α with discrete β particles distributed either along grain boundaries or within the matrix is expected [9] to possess superior corrosion resistance. The proportion and morphology of both the constituents need to be tailored to achieve the best combination of corrosion and mechanical properties.

In the case of Ti–Ta–Nb alloys, a systematic study on the microstructures that form during various thermal and thermo-mechanical treatments, and their consequence on corrosion behavior, has not been carried out so far. Hence, the present paper attempts to identify the (i) optimum microstructure for better corrosion resistance and (ii) the means to achieve the same by various combinations of thermal and thermo-mechanical treatments on a developmental Ti–5%Ta–1.8%Nb alloy.

2. Experimental

The Ti–5%Ta–1.8%Nb alloy was obtained from Nuclear Fuel Complex, Hyderabad [10], in the form of an ingot of 150 mm and rods of 25 mm diameter in two different metallurgical conditions. The two conditions are referred to as 'β annealed' and 'thermo-mechanically processed' (TMP) conditions respectively, the details of which are described in the subsequent sections. The chemical composition of the alloy is given in Table 1. The β annealed alloy was subjected to a series of thermal and thermo-mechanical treatments in different phase fields, a brief description of which is given below. The treatments with appropriate codes are also summarized in Table 2.

(a) Thermal treatments:

(i) Two-stage treatment: A sample of dimensions 5 mm diameter and 10 mm length was solution treated for 1 h at 1273 K in the β phase field, slow cooled to 1103 K and held for 2 h and further furnace cooled to room temperature. This treatment was carried out in a HTC-HFDSC 16 (SETARAM) differential scanning calorimeter with controlled cooling rates.

(ii) Direct treatment (in vacuum) at 1103 K, high in the two-phase field for 2 h followed by furnace cooling.

(iii) Direct treatment (in vacuum) at 973 K, low in the two-phase field for 72 h followed by water quenching.

(b) Thermo-mechanical treatment: The thermo-mechanically processed alloy (TMP alloy) was received from NFC in the form of 25 mm rods after the following treatments. The β annealed alloy was subjected to a series of thermal and mechanical processes which included hot extrusion in the two-phase field (1103–1113 K), β quenching, tempering, cold swaging and

Table 1
Composition of the alloy

	Elements							
	Ta	Nb	Fe	O	N	C	H	Ti
Amount	4.39 wt%	1.85 wt%	263 ppm	500 ppm	47 ppm	125 ppm	9 ppm	Balance

Table 2
Details of heat treatments employed in the present study

S. no.	Temperature, K	Time, h	Mode of cooling	Code
1	As-received		Slow cool	A
2	Stage 1:1273 K	2	Programmed slow cool to 1103 K	B
	Stage 2:1103 K	2	Furnace cool	
3	1103 K	2	Furnace cool	C
4	973 K	72	Water quench	D
5	TMP			E
6	Stage 1: 1223 K	2	Water quench	F
	Stage 2: 1113 K	2	Water quench	

Table 3
Techniques used in this study and their operating conditions

Technique	Equipment	Operating conditions
X-ray diffraction	Philips PW-1730	CuKα radiation
Microhardness	Leitz Miniload-2	Load of 100 g
Optical microscopy	Leica MeF4A	Bright field
Scanning electron microscopy	Philips XL 30	20–30 kV
Analytical transmission electron microscopy	Philips CM 200 with SUTW EDAX and DX4 analyser	120–200 kV
Differential scanning calorimetry	HTC-HFDSC 16 (SETARAM)	Heat flux DSC

intermittent stress relieving treatments in the range of 903–923 K.

The alloy received in the above condition was further subjected in the laboratory to a reverse treatment consisting of a two-stage process; the first step was a β quench from 1223 K followed by an isothermal treatment at 1113 K in the two-phase field, in order to understand the significance of thermo-mechanical processing.

The specimens for optical, scanning electron microscopy were prepared by standard metallographic methods. Optical and scanning electron microscopy were carried out using a Leica MeF4A and Philips XL30 ESEM microscopes respectively. Transmission electron microscopy on thin foils was carried out using a Philips CM200 with energy dispersive spectrometer (Super Ultra Thin Window) and DX4 Analyser. Identification of the phases was carried out using a Philips (PW-1730) X-ray diffractometer with CuKα as incident radiation. The operating conditions used for the different techniques are given in Table 3.

3. Results

This study had a twofold objective namely (a) identification of the microstructure suitable for high corrosion resistant performance and (b) development of thermal/thermo-mechanical treatments to obtain this desirable microstructure. The results are presented in this section as follows: Section 3.1 presents a microstructural analysis to identify the desirable, optimum microstructure based on corrosion rates. Detailed characterization of the β annealed alloy is described in Section 3.2. The modification of this structure by a series of treatments is described in Section 3.3, based on which the method to arrive at the desired structure is deduced. Uniqueness of the processing route has been highlighted in Section 3.4 based on the stability of the desired structure.

3.1. Identification of optimum structure

The microstructural observations of the alloy in two conditions, namely the initial 'β annealed' and 'thermo-mechanically processed' (TMP) are presented in this section. Fig. 1(a) shows the microstructure of the alloy in the as-received 'β annealed' condition. Large grains of β, with sizes as large as 1.7 mm are observed with a continuous layer of α along the boundaries. The rapid growth of β grains in Ti alloys is a problem frequently encountered, especially in weldments [11]. It was observed that the prior β grains had several colonies of 'transformed β' with uniform acicular structure. The average size of the colony was about 54 μm. Despite a uniform distribution of the transformation products with a lamellar morphology, the hardness of the alloy was found to be only 182 VHN. Similar structures called 'transformed β structure' in Ti alloys have been shown to be a product of Widmanstatten transformation of β,

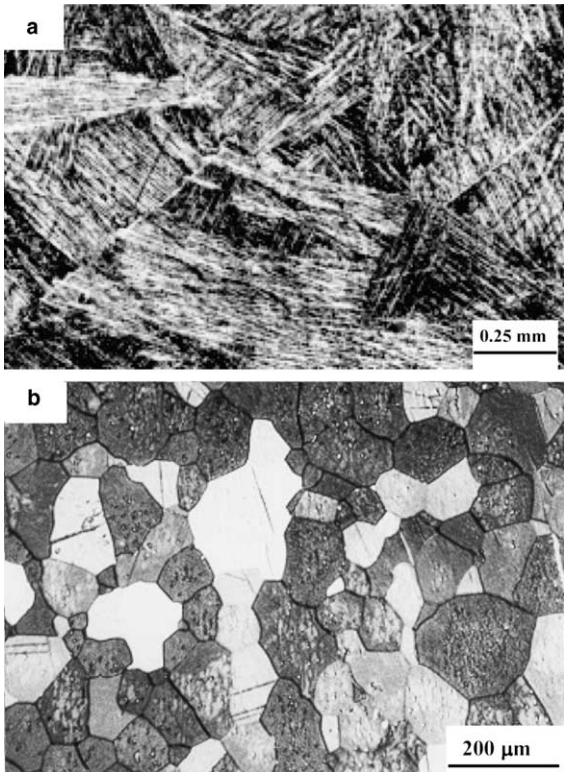

Fig. 1. Optical micrographs of the alloy received in the two conditions namely (a) β annealing showing uniformly acicular 'transformed β structure' with α colonies inside the prior β grains and (b) thermo-mechanical processing showing an uniform equiaxed structure.

during cooling from the β phase field [12]. Fig. 1(b) shows the microstructure of the TMP alloy. This structure consisted of a large volume of fine equiaxed grains with a distribution of fine particles. The size of the equiaxed grains range from 12 to 15 μm.

The corrosion behaviour of the alloy with the above two structures have been studied in detail [13,14]. The average corrosion rates in boiling nitric acid of the alloy with the two structures namely lamellar and equiaxed structures was found to be 1.49 and 0.26 mpy respectively. Such a large difference in the corrosion rates clearly suggests that the alloy with equiaxed grain structure exhibits superior corrosion behavior in comparison to the structure with lamellar morphology. Such an equiaxed structure has also been reported to show lower corrosion rate compared to an acicular structure in case of commercially pure Ti [9]. It is to be recalled that the Ti–5Ta–1.8Nb alloy in the as-cast/β annealed condition possesses an acicular structure. Hence, a processing route needs to be developed that would yield an equiaxed structure starting from an acicular one.

The initial β annealed alloy was characterized in detail to identify the microstructural features, following which it was subjected to a series of thermal and thermo-mechanical treatments, resulting in a variety of microstructures, culminating in the desired equiaxed structure, the details of which are discussed in the following sections.

3.2. Characterization of initial microstructure in 'β annealed' condition

Fig. 2(a) shows the optical microstructure of the β annealed alloy at a magnification higher than Fig. 1(a). In addition to coarse prior β grains and α colonies, the presence of continuous film of α along the prior β grain boundaries is observed. It has been reported [15] that grain boundary α is the first phase to form while cooling the high temperature β phase, due to ease of nucleation. The presence of such grain boundary α is deleterious causing embrittlement in some of the Ti-based alloys [16]. The width of the grain boundary α is found to be about 2.7 μm. However, its further growth into β is prevented by the onset of competing Widmanstatten transformation of β, as the alloy is cooled further. This transformation of the remaining β results in the formation of alternate lamellae of α and β, leading to the observed acicular morphology of the transformation products.

The confirmative, crystallographic evidence for the presence of the cubic β and hcp-α can be obtained only by resorting to diffraction experiments, either using X-rays or electrons. In the present study, X-ray diffraction result was not conclusive [17] though it suggests the presence of β phase. This is due to the overlapping of $(1\,1\,0)_\beta$ peak of 100% intensity at 38.4° with the $(0\,0\,2)_\alpha$ peak with 30% intensity. The other peaks of β phase could not be observed probably due to low

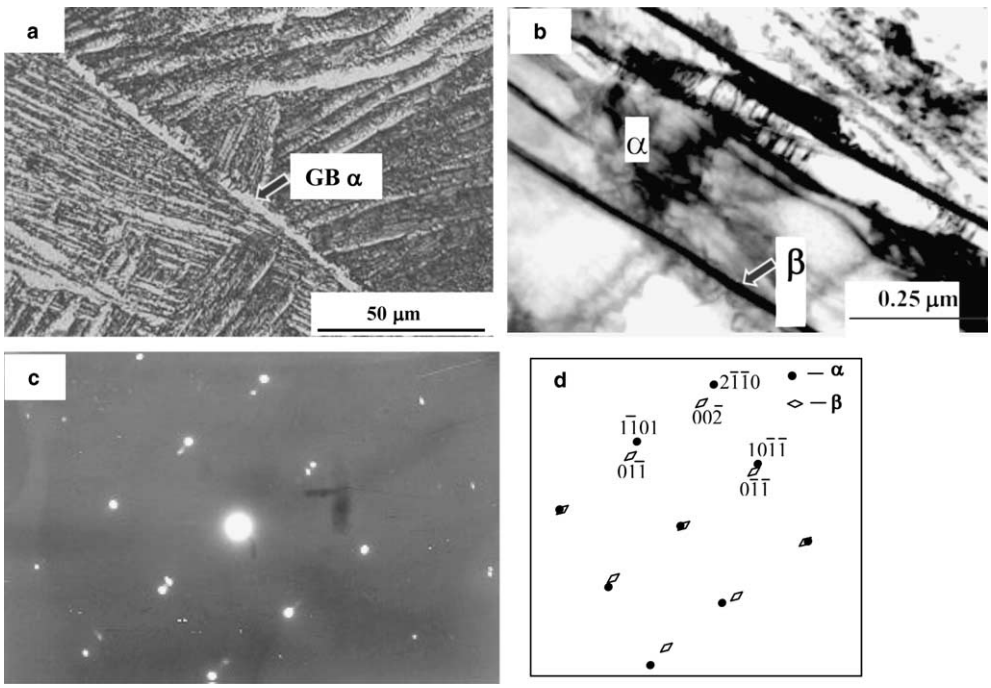

Fig. 2. Microstructures of the β annealed alloy showing (a) grain boundary α decorating the prior β boundaries (arrow marked) and acicular transformed β within; (b) well-resolved individual lamellae of the two phases; (c) selected area diffraction (SAD) pattern from both α and β phases along $[0\,1\,\bar{1}\,1]$ and [1 0 0] zone axis respectively and (d) key to SAD pattern in (c).

amounts of β and the inherently low diffracted intensity of higher order reflections. Hence, electron microscopy of thin foils of the β annealed sample was carried out.

Fig. 2(b) shows the transmission electron micrograph of the β annealed sample with well-resolved lamellae. Analysis of the selected area diffraction (SAD) pattern taken from both the lamellae (Fig. 2(c)) with its key in Fig. 2(d), confirms the presence of α phase along $[0\bar{1}\bar{1}1]$ and β phase along [100] zone axis respectively. This confirms that the microstructure consists of alternate lamellae of α and β, referred in literature as transformed β [12]. It is also observed that the **g** vectors of $(110)_\beta$ and $(0001)_\alpha$ are nearly along the same direction, suggesting $(110)_\beta \| (0002)_\alpha$, the well-known Burger's orientation relation [18]. The orientation relationship is known to be as follows:

$$(110)_\beta \| (0002)_\alpha$$
$$\langle 111 \rangle_\beta \| \langle 2110 \rangle_\alpha$$

There was a large variation in the width of the individual lamella from one region to another. The width was measured to be in the range of 0.1–1.06 μm and 0.01–0.25 μm for α and β respectively. The amount of retained β phase estimated by conventional image analysis procedures was found to be about 12–15%. In order to identify if there was solute repartitioning between α and β, energy dispersive spectroscopy (EDS) analysis was carried out. Fig. 3(a) and (b) shows the EDS spectra from α and β phases respectively. An observable increase in the amount of Nb and Ta in β phase, in comparison to the α phase is clearly seen. This confirms that there has been solute repartitioning between α and β phases. The above experiments showed that the as-received 'β annealed' alloy consists of a continuous film of α along the prior β boundaries and alternate lamellae of α and β phases within.

3.3. Selection of processing route to obtain a microstructure with improved corrosion resistance

It follows from Section 3.1 that an equiaxed microstructure needs to be obtained since the corrosion rate

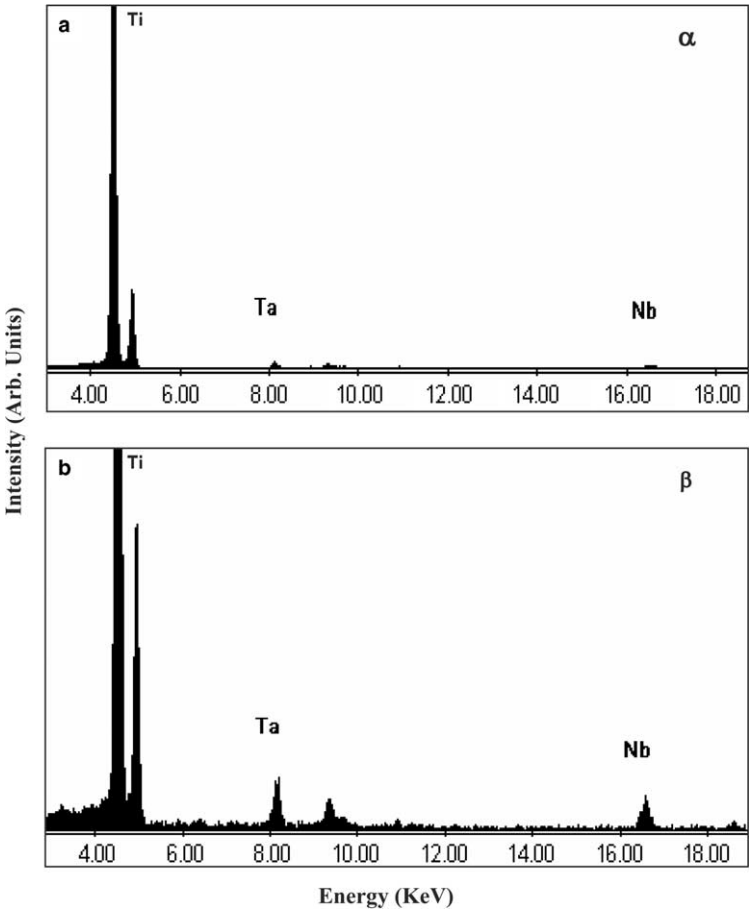

Fig. 3. (a, b) EDS spectra from the α and β lamellae showing enrichment of Ta and Nb in β phase in β annealed alloy.

of the alloy in this condition was observed to be lower than the lamellar structure. Hence, the β annealed alloy was subjected to a series of thermal/thermo-mechanical treatments and the microstructural evolution of the alloy during these treatments studied, results of which are presented in the following subsections.

3.3.1. Microstructural changes during isothermal treatments in α + β phase field

The formation of primary α during isothermal treatments in the two phase field either directly or by a two-stage process was studied. A controlled two-stage heat treatment (treatment B – 1273 K slow cooled to 1103 K followed by furnace cooling) was carried out in a differential scanning calorimeter, as described in Section 2. The resultant microstructures are shown in Fig. 4. The SEM micrograph in Fig. 4(a) shows the presence of grain boundary α along prior β boundaries and a lamellar transformed β structure formed during cooling from the β phase field. This transformed β structure could have formed during either of the cooling stages (1273–1103 K or 1103 K to room temperature). Fig. 4(b) shows the presence of coarse primary α (marked as α_p in Fig. 4(b)) with morphology of long aligned plates. These are expected to have formed from the transformed β structure during the aging at 1103 K. While cooling further, the remaining high temperature β undergoes Widmanstatten transformation resulting again in a matrix of transformed β (Fig. 4(b) and (c)).

The presence of large β grains (Fig. 4(c)) of the order of 2 mm is attributed to the high rate of grain growth at 1273 K [15]. The average size of a α colony was found to be 66 μm, coarser than that of the β annealed alloy (54 μm), which is due to the slow cooling from 1273 K. The width of grain boundary α was 12 μm, which was significantly higher than 2.7 μm for the β annealed sample. The specimen showed a uniform hardness of about 155 VHN. The microstructural parameters and hardness values reflect the 'long time' available for the growth of grain boundary and lamellar α during cooling from 1273 to 1103 K. These parameters are listed in Table 4.

Fig. 5(a) shows the transmission electron micrograph of the same sample, revealing the well-resolved individual lamellae. The SAD patterns from the individual lamellae are shown in Fig. 5(b) and (c), analysis of which has identified them as bcc-β and hcp-α phases. The width of α and β lamellae were in the range 1–4 and 0.4–0.8 μm, respectively, which are an order of magnitude higher than that of the β annealed sample. However, the volume fraction of retained β remained the same as 12–14%. Fig. 6(a) and (b) shows the EDS spectra from α and β phases. The higher amount of Ta and Nb in β relative to α phase provides direct evidence for solute repartitioning, during the β → α + β transfor-

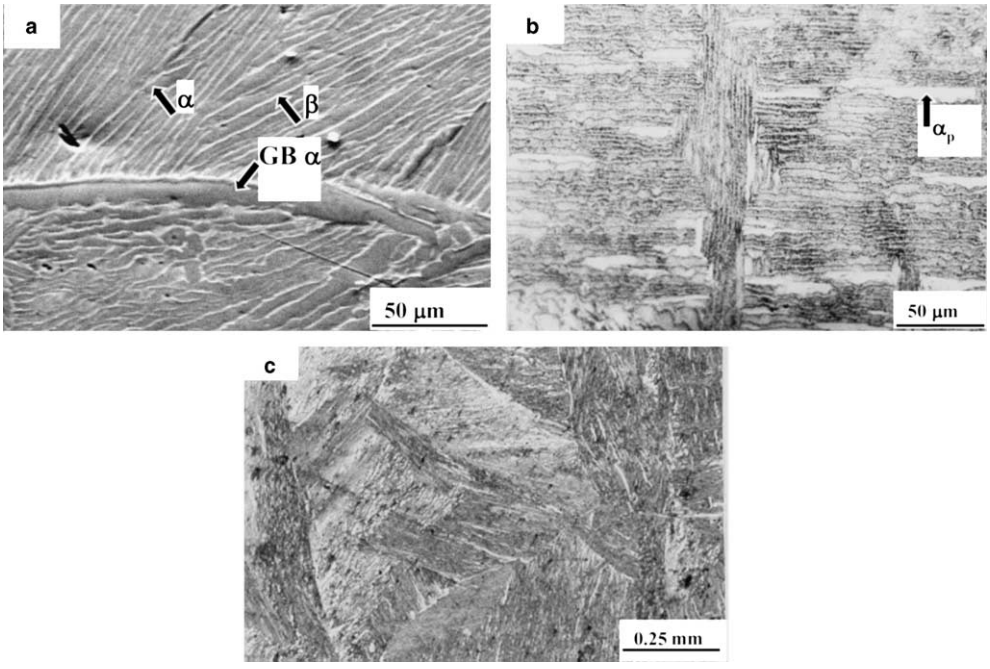

Fig. 4. Microstructures of the alloy subjected to treatment B: (a) SEM micrograph showing a transformed β structure with alternate lamellae of α and β and a continuous film of grain boundary α (arrow marked) formed on prior β boundaries; optical micrographs showing formation of (b) coarse plates of primary α (α_p – arrow marked) during treatment in α + β phase field and (c) transformed β during cooling from two-phase field.

Table 4
Variation of microstructural parameters and hardness for different heat treatments

Code	Amount of retained β, %	Prior β grain size, mm	Grain size of α, μm (∑±10%)		Width, μm (∑±10%)				Hardness, VHN
			Primary α	α colony	GB α	α lamellae	β lamellae	β nodule	
A	12–14	1.7	–	54	2.7	0.1–1.06	0.01–0.25	–	182
B	12–14	2.2	–	66	12.69	1–4	0.4–0.8	–	155
C	11–12	1.92	–	62.5	5.0	2.96	0.37–1	–	140
D	5	1.64	–	334.4	4.4	1.5	–	–	137
E	5	–	12	–	–	0.3–0.4	–	0.1–0.6	165
F	2	0.20	–	–	–	–	–	–	195

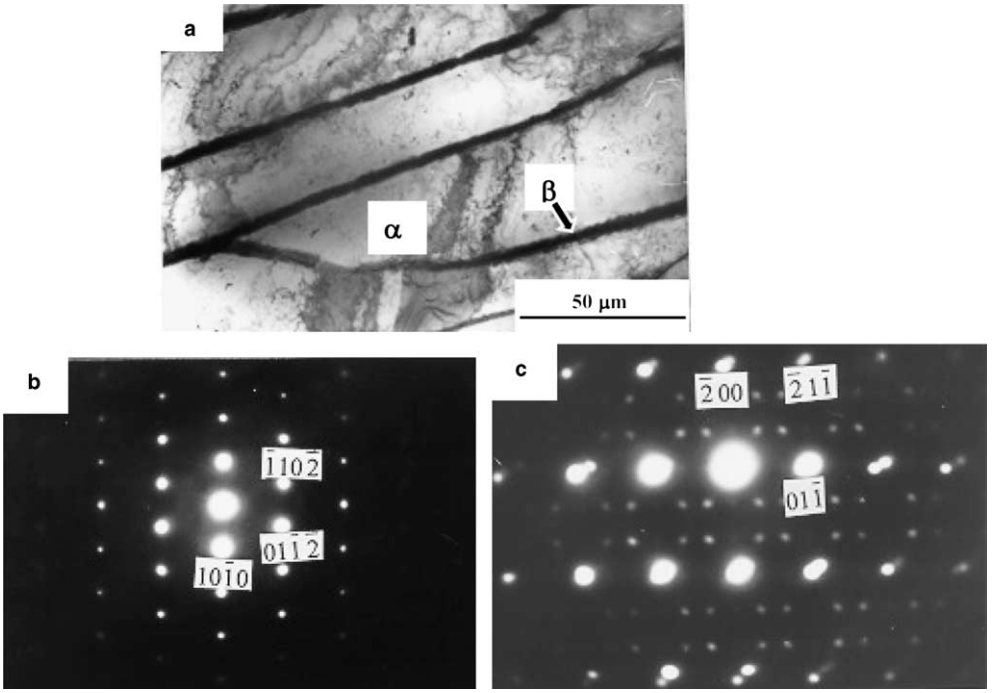

Fig. 5. (a) TEM micrograph of the same sample as in Fig. 4, showing well-resolved individual lamellae of α and β, (b, c) SAD patterns confirming α and β phases along zone axes $[\bar{2}4\bar{2}3]$ and [0 1 1] respectively.

mation. The enrichment of Ta in the β phase is further demonstrated in the Ta X-ray map in Fig. 6(c).

The above observations show that subjecting the β annealed Ti–Ta–Nb alloy to a two-stage treatment, first in β and further in α + β phase fields results in the following transformations:

It was anticipated that the β phase that formed at 1273 K would transform to α on slow cooling, to the extent depending on the 'time of stay' between β transus (1143 K) and 1103 K. Further, it was expected that aging at 1103 K would result in equiaxed α grains, followed by transformation of the remaining high

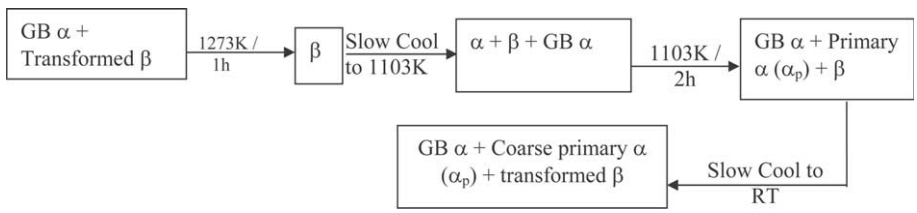

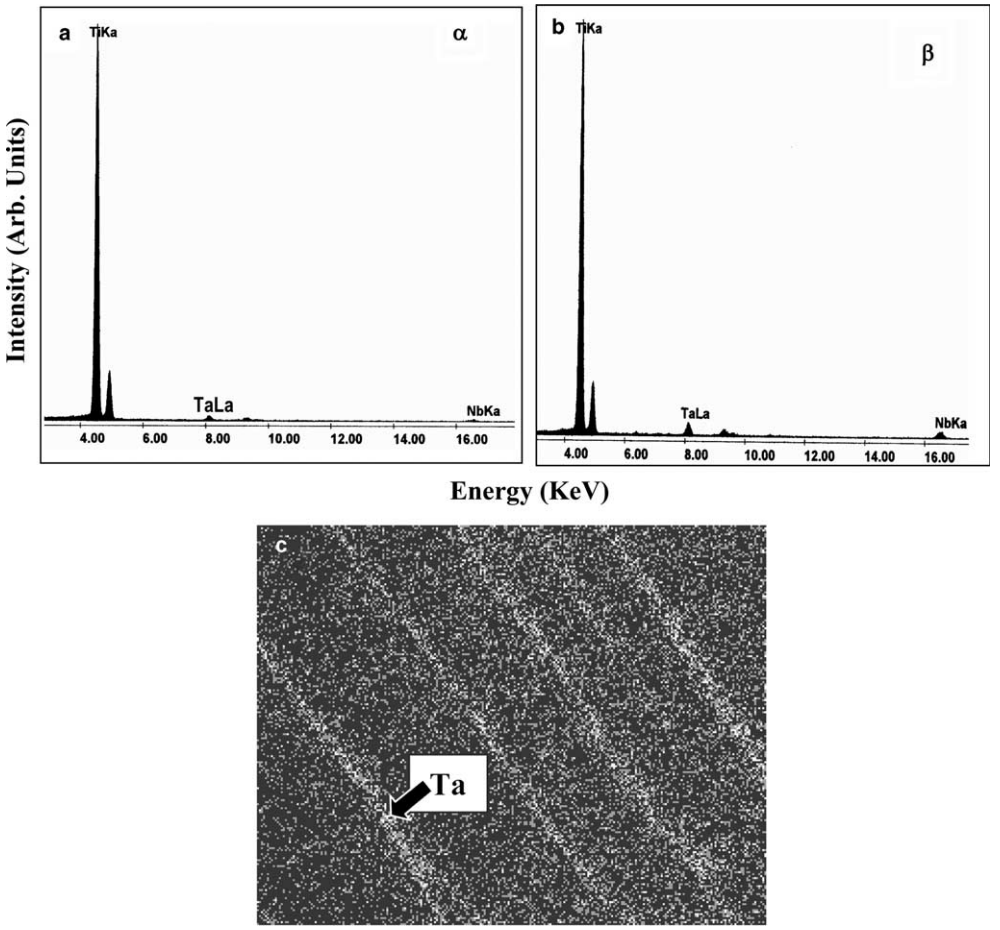

Fig. 6. (a, b) EDS spectra from α and β phases, showing enrichment of Ta and Nb in β and (c) X-ray map of Ta from the same region, showing the repartitioning of Ta between α and β phases.

temperature β to lamellar α + β. However, the above experiments have shown the following results: (a) Primary α nucleate and grow in the β grains in the form of plates only; (b) Primary α remains stable while the remaining β phase decomposes into lamellar transformed β during cooling.

The next attempt was to treat the β annealed alloy directly at 1103 K – a temperature high in the α + β phase field, followed by slow cooling. The pre-existing α lamellae were expected to grow at this temperature and possibly result in an equiaxed structure. Fig. 7 shows the optical micrograph of this sample. The formation of several colonies of α inside the prior β grains is clearly revealed. Well-aligned lamellae within the α colonies and coarse grain boundary α along prior β boundaries are also observed clearly. There was no significant change in the microstructural parameters and hardness, as can be seen from Table 4. The above studies show that, although treatment in the α + β phase field pro-

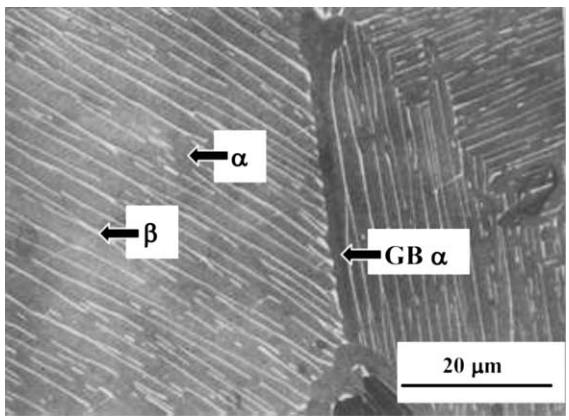

Fig. 7. Microstructure of the Ti–5%Ta–1.8%Nb alloy slow cooled from 1103 K showing transformed β structure and grain boundary α. Several colonies of α are seen within a β grain.

duced large amounts of α its morphology remained acicular.

Another attempt to obtain the desired structure was made by treating the β annealed alloy for long duration at 973 K – low in the two-phase field. The intention was to nucleate a large number of primary α grains, which would grow into polygonal α, during the prolonged treatment. Fig. 8(a) shows the optical micrograph of the resultant structure. The formation of coarse α colonies with jagged boundaries within a prior β grain is clearly revealed. These α colonies termed as 'serrated α' [19], have been observed to form in a matrix of transformed β. At higher magnification (Fig. 8(b)), incomplete conversion of β lamellae within the serrated α colony is observed. Since the volume fraction of retained β is low, it is expected to have a high solute enrichment, which inhibits the transformation of β to α′. The large size of the α plates is attributed to the growth of α lamellae at 973 K, during which the transformed β with lamellar morphology breaks up, resulting in the partial conversion of β to α. The observation of grain boundary α in very few regions could be due to its consumption during the growth of α, resulting in an irregular serrated morphology. The transformation at 973 K can be summarized as follows:

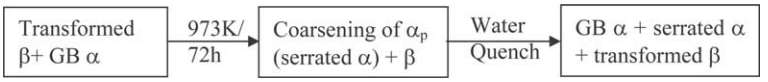

The above observations clearly demonstrate that thermal treatments in the two-phase field are not adequate to obtain the desired duplex microstructure in an alloy, whose initial microstructure consists of grain boundary α and transformed β.

3.3.2. Microstructural changes during thermo-mechanical treatments

Since the isothermal treatments of the β annealed alloy did not yield the desirable structure, the alloy was subjected to a series of forming operations to process the ingot into a rod form. The stages included a hot extrusion high in the two-phase field, a β quenching treatment and a series of cold swaging operations with intervening stress relieving treatments at low temperature [10]. The alloy received in the above condition showed a microstructure consisting of equiaxed grains as described in Section 3.

An extensive microscopy investigation was carried out to identify the morphological and microchemical details of the coexisting phases in the alloy. The SEM micrograph in Fig. 9(a) shows a microstructure consisting of a uniform distribution of equiaxed grains. The presence of globular precipitates within the α grains is seen clearly. These precipitates were observed to have sizes ranging from 100 to 500 nm. The fine size of the precipitates necessitated a detailed examination of the structure by transmission electron microscopy. Fig. 9(b) and (c) shows the presence of α with two types of morphologies, namely equiaxed and acicular respectively. The precipitates were observed as isolated globular particles distributed along the boundaries of either equiaxed α (Fig. 9(b)) or acicular α (Fig. 9(c)). The size and volume fraction of these particles ranged from 0.1 to 0.6 μm and 3–5% respectively. Analysis of the SAD pattern (inset in Fig. 9(b)) from an isolated particle along the grain boundary shows that it is β phase oriented along [1 1 1] zone axis. The solute redistribution between α and β phases is shown in the EDS spectra in Fig. 10(a) and (b). Higher amount of Ta and Nb is clearly observed, confirming the solute rich nature of the β phase. EDS spectra from a number of such particles showed an observable amount of dissolved iron in a few particles (Fig. 10(c)). This is probably due to the low amount of iron (~260 ppm) present in the alloy, partitioning itself preferentially into the β phase, being a strong β stabilizing element.

The observation of isolated fine β particles along lath boundaries and substructures in the α matrix in the present case suggests that the β phase has precipitated from a supersaturated solution during tempering of martensite. This can be understood in the light of the β quenching and tempering treatments that the alloy is subjected to after the initial large hot deformation of the ingot [10]. It is also reported that in β isomorphous alloys, the supersaturated martensite (α′) decomposes directly to the equilibrium α and β phases, where the β precipitates nucleate heterogeneously at the lath boundaries and internal substructures [20]. During further forming operations both α and β phases undergo deformation. During stress relieving treatment, the deformed α undergoes recrystallization, resulting in large volume fraction of equiaxed α grains, while the deformed β particles get annealed of the internal defects. The occasional presence of acicular α in the microstructure suggests that recrystallization is incomplete.

The above results confirm that cold deformation of a β quenched and tempered alloy, followed by low temperature anneal in the two-phase field would lead to the formation of the desired duplex microstructure. The amount of constituent phases in the duplex structure can be further tailored by carrying out selective treatments, which are under study.

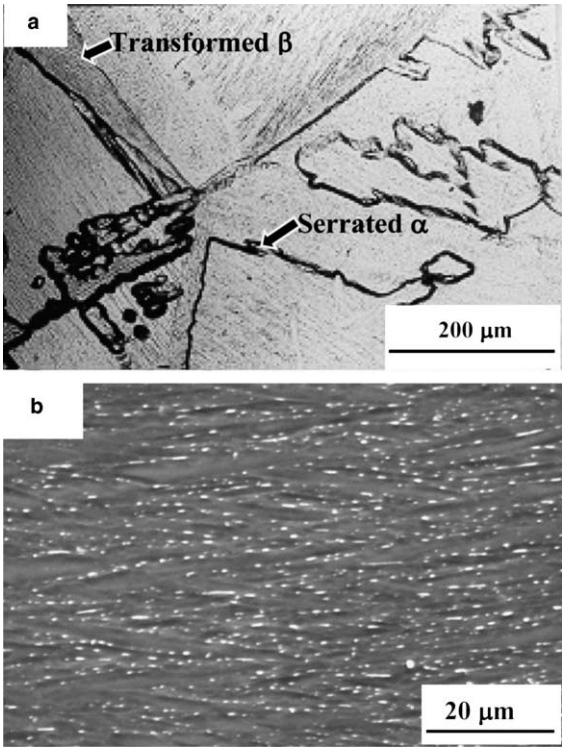

Fig. 8. Microstructure of Ti–5%Ta–1.8%Nb alloy, annealed for 72 h at 973 K, low in the two-phase field, and water quenched (treatment E) showing (a) coarse α colonies with jagged boundaries termed as serrated α colonies along with transformed β and (b) partial conversion of the β lamellae within serrated α colony.

3.4. Stability of the duplex structure

In order to recognize the exclusive role of mechanical working in obtaining a structure with large volume fraction of equiaxed α, a two-stage simulation treatment (treatment F – holding for 2 h at 1223 K and water quenching followed by a similar treatment at 1113 K) was carried out, as described in Section 2. The optical micrograph (Fig. 11(a)) of the alloy subjected to the above treatment showed a structure completely different from the TMP alloy. Large β grains with fully acicular structure were observed. No evidence for grain boundary α was observed. This shows that the prior history of the alloy consisting of an equiaxed α matrix is completely erased during the β quenching. The second treatment in two-phase field yielded α only in an acicular morphology. Further analysis showed the precipitation of fine particles along the lath boundaries (Fig. 11(b)). This is attributed to the tempering of α′ that formed during β quenching. The TEM micrograph of the alloy after the two-stage treatment (Fig. 11(c)) shows the presence of fine precipitates. Analysis of the SAD pattern (inset in Fig. 11(c)) confirms β along [0 1 1] zone axis. The DF micrograph (Fig. 11(d)) with $(0\,1\,\bar{1})$ reflection shows the precipitation of β along lath boundaries and dislocation substructure. Another interesting observation (Fig. 11(e)) was the presence of fine α′ laths at the triple points of prior β grains. The EDS spectra from these α′ laths (Fig. 11(f)) showed higher amount of Ta and Nb (characteristic of β phase) in comparison to the tempered martensite matrix. The presence of α′ suggests that the β phase had formed along the triple points of prior β grains during the tempering process in addition to the precipitation along lath boundaries and internal structures. The transformation of coarse β along the grain boundary triple points into α′ in contrast to their retention as fine precipitates along lath boundaries and dislocation substructures is attributed to the size effect [21], rather than the effect of composition. These results show that the alloy after the two-stage treatment consists of a mixture of fine precipitates along lath boundaries and dislocation substructures and α′ in a matrix of tempered martensite. The above experiment again proves that thermal treatment alone is not adequate to obtain the desired structure, thus highlighting the role of mechanical working. It is understood that the equiaxed α grains nucleate and grow by recrystallization of the deformed α phase, while the fine, globular β precipitates form by tempering of the martensite, prior to cold deformation.

The above set of experiments offered important information with respect to processing of Ti–Ta–Nb alloys: The desirable microstructure for corrosion applications is identified as the duplex structure. This is evident from the corrosion rate evaluated for the alloy with duplex structures [13], which is only 20% of the values reported for acicular structures [10]. Of the various combinations of treatments carried out for this alloy, like, β anneal, α + β treatments with different process conditions, and deformation followed by stress relief, with an intervening β quench, the last one was found to offer the duplex microstructure of equiaxed α with random distribution of isolated fine, globular particles of β. The advantage that is obtained by deformation and stress relieving treatment will be lost, even if inadvertently the alloy is exposed to temperatures exceeding the β transus (~1133 K). Hence, the final processing step for applications in high corrosion environment should be only deformation and stress relieving treatment, taking care that the temperature is well within the α + β phase field. Though such a stringent requirement can be met for the wrought alloy, the situation in a weldment is entirely different, wherein a variety of microstructures form, depending on the thermal cycles experienced by each region. It remains to be seen whether it is beneficial to avoid transformed β completely as an extreme case,

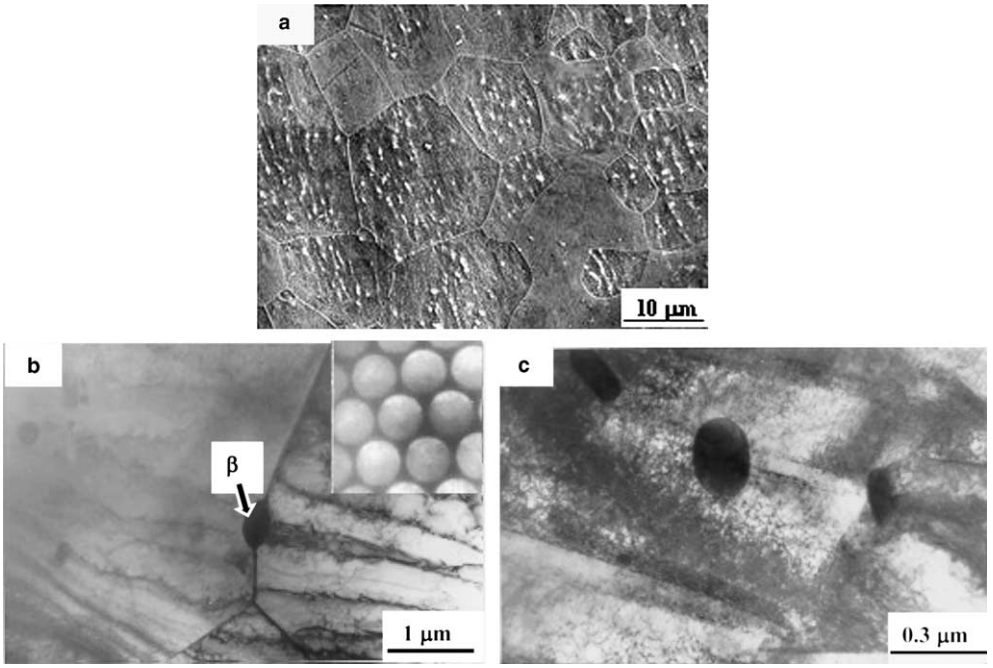

Fig. 9. (a) SEM micrograph of the Ti–5%Ta–1.8%Nb alloy in the TMP condition showing the distribution of nodular β in an equiaxed α matrix; evidence for the distribution of β as isolated, globular particles along (b) grain boundaries of recrystallized primary α and (c) tempered martensitic lath boundaries. The microdiffraction pattern shown as inset in (b) confirms the presence of $[1\,1\,1]_{\beta}$.

and instead choose martensitic α'. This selection will depend on the extent to which corrosion rates are influenced by the galvanic effect of transformed β and strain induced corrosion due to martensitic α′. The microstructural heterogeneities in the weldments of this alloy and its effect on corrosion behavior are under detailed study.

4. Discussions

The results presented in Section 3 have enabled the identification of the microstructure suitable for corrosion applications in a Ti–5%Ta–1.8%Nb alloy and the processing route to achieve this structure. In addition, the results contain useful information on the influence of microstructure on corrosion behavior of the alloy, mechanisms of phase transformations and role of deformation during various treatments, which will be discussed in this section.

4.1. Identification of microstructure desirable for exhibiting good corrosion resistance

As seen from Section 3.1, the Ti–Ta–Nb alloy in TMP condition with a structure of equiaxed α and random particles of β showed a better corrosion resistance than the β annealed alloy. The latter microstructure consisting of alternate lamellae of α and β phases, led to formation of microgalvanic cells at the interface and hence is deleterious [9]. In the absence of such a periodic microchemical variation as in the case of TMP alloy, it was expected that tendency for formation of microchemical galvanic cell would be minimized, resulting in good corrosion resistance. Hence, in order to obtain large amount of equiaxed α phase, the β annealed alloy was subjected to different thermal treatments at progressively lower temperatures in the $\alpha + \beta$ phase field. However, each of the thermal treatments resulted only in the formation of the 'undesirable' microstructure consisting of acicular products, whose size varied depending on the heating and cooling conditions.

Characterization of the alloy during the development of processing flow chart, consisting of several stages of extrusion, swaging and stress relieving treatments, showed that equiaxed α phase formed by recrystallization of a deformed alloy, while the β phase distributed itself as nodular particles during an intermediate β quenching and tempering process. It was therefore inferred that thermo-mechanical processing of the β annealed alloy resulted in a desirable microstructure while thermal treatments always produced the wrong microstructure.

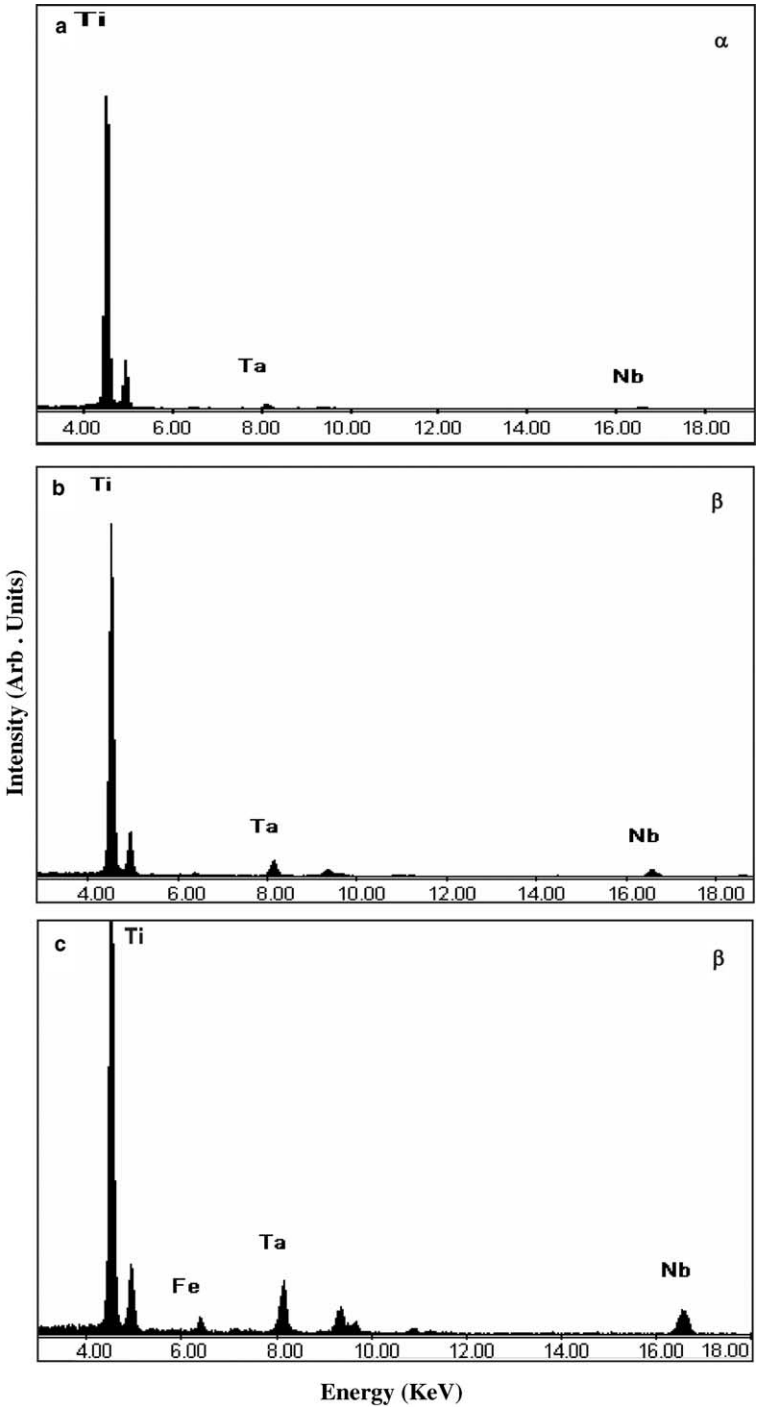

Fig. 10. EDS spectra from α and β phases in TMP condition showing (a) solute lean α phase, (b, c) enrichment of Nb and Ta in β phase. Segregation of Fe in β phase is seen occasionally (c).

The above discussion on β annealed and TMP alloys shows that microstructure plays a crucial role on the corrosion behaviour. Additional experiments to further enhance the corrosion resistance of TMP alloy by tailor-

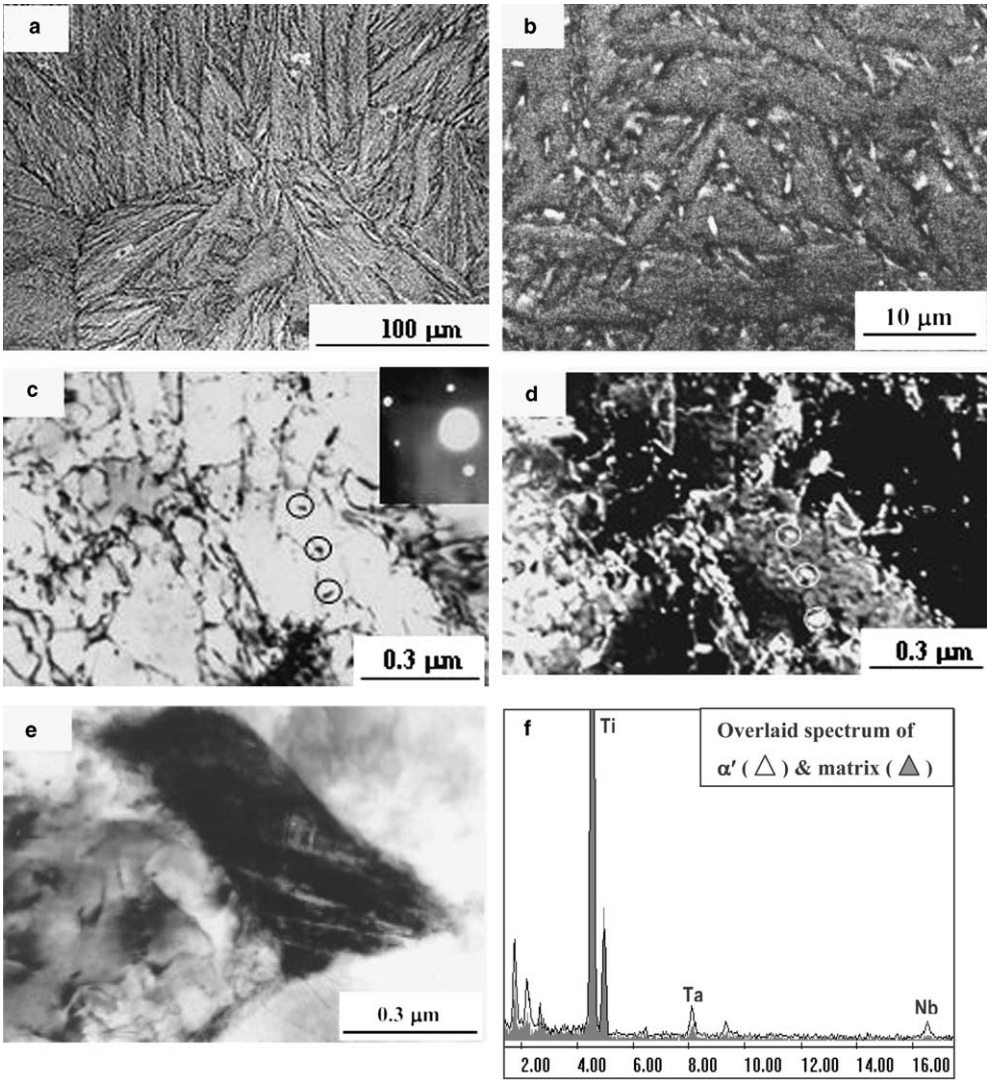

Fig. 11. Microstructures of the alloy treated above T_β (treatment F) showing (a) a fully acicular product, (b) SEM micrograph showing fine precipitates on lath boundaries, (c, d) TEM BF and DF micrographs showing precipitation of fine β (circled) at substructures of α′. SAD inset in (c) confirms β along $[0\,1\,1]_\beta$, (e) formation of α′ at the grain boundary triple points and (f) EDS spectra from these α′ regions showing higher amount of Ta and Nb as compared to tempered martensite matrix.

ing the microstructure by suitable heat treatments [22] showed that the distribution of β phase as fine particles in an equiaxed α matrix offered the best corrosion resistance. This is attributed to the enhanced stability of the passive oxide film offered by the Ta- and Nb-rich fine β particles, which in turn reduces the dissolution rate of titanium and amount of dissolved titanium ions that would act as inhibitor. Having identified the optimum microstructure, the transformations in the alloy during different treatments to obtain such a microstructure will be discussed in the subsequent sections.

4.2. Microstructural evolution during thermal treatments

The results in the previous section have shown that the initial structure of the alloy in the 'as-received' ingot form is the transformed β structure, consisting of alternate lamellae of α and β, formed by slow cooling. Such a structure when again heated above the β transus and cooled, showed the following features: (i) Rapid growth of parent β grains, resulting in very large (as high as 2 mm) prior β grains and (ii) product consisting of either

martensite or Widmanstatten α (lamellar α and β) with grain boundary α depending on whether the alloy is quenched or annealed respectively.

The transformations can generally be summarized as follows [23]:

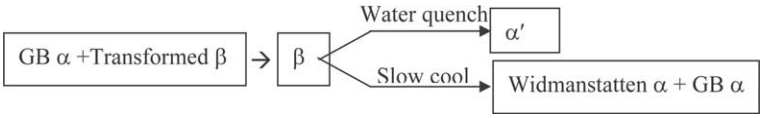

Rapid grain growth in Ti-based alloys has been reported in several studies [11,15]. This has been attributed to the low values of activation energy ($Q \sim 95$ kJ/mol) for self-diffusion, responsible for grain growth in bcc Ti, compared to other metallic systems like α and γ Fe, with Q values of 239 and 270 kJ/mol respectively [15]. In fact, Sundaresan et al. [11] have identified rapid grain growth as one of the major problems in weldments of Ti and have discussed methods for refinement of β grains.

Though α with several morphologies, like lamellar or acicular or basket weave have been observed, it has been understood that they all are essentially products of a Widmanstatten transformation during cooling of β, at different rates. But none of the above types of α is desirable for corrosion applications. In fact, all forms of α interwoven with β lamella/plate act as effective galvanic couples leading to increased rate of corrosion. The grain boundary α, on the other hand, behaves like the precipitate free zones (PFZ) in over aged Al alloys [24]. This phase has a negative influence on some of the mechanical properties like fracture strain, HCF properties, K_{1C} and cracks are known to nucleate easily along the grain boundary α. It has been possible to eliminate the grain boundary α in Ti alloys by deforming the alloy below β transus [24]. The transformation sequences observed during the treatments of Ti–Ta–Nb in α + β phase field either directly or in two stages are summarized as follows:

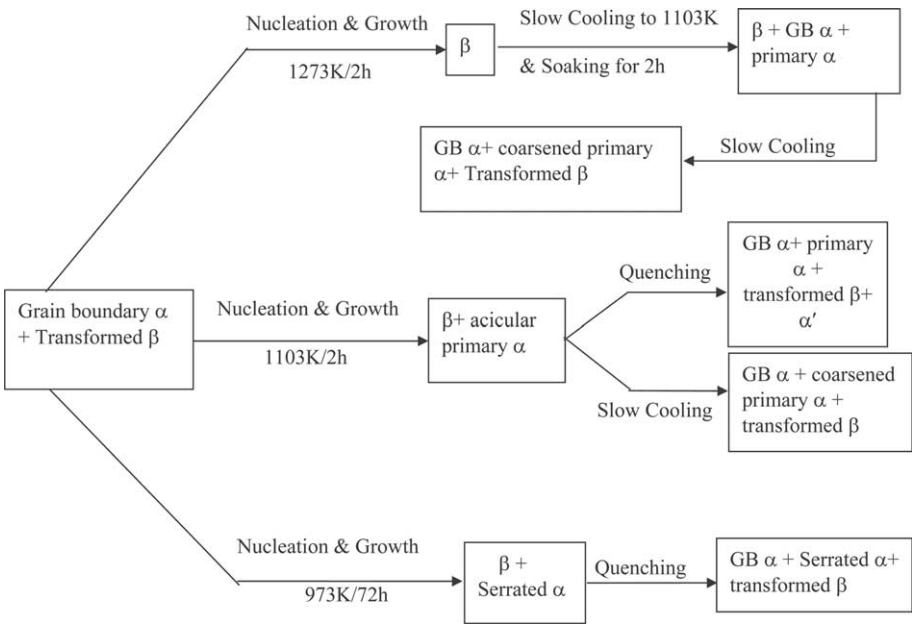

The growth of primary α (α_p) in the two-phase region during aging is found to be always in the form of coarse platelets, irrespective of whether they are nucleating and growing within a β grain or transformed β matrix. Direct aging of the transformed β in the duplex field, results in gradual coarsening of the pre-existing acicular α to yield the amount of α characteristic of the aging temperature. Once the required volume fraction of α_p as dictated by the temperature and time has grown, the remaining β, undergoes one of the transformations listed above, to

yield either α' or α_W with grain boundary α, depending on the cooling rate. Generally, it is known that the growth of recrystallized grains is sluggish in a mixed matrix of two phases. Harold Margolin and Cohen [25], while studying the kinetics of grain growth in a Ti alloy with equiaxed α, has shown that higher aging temperatures in the two-phase field, retard the growth of primary α, due to increase in the volume fraction and size of β, which anchor the α boundaries effectively.

4.3. Microstructural evolution during deformation and stress relieving treatment

Extensive literature regarding thermo-mechanical processing is available for many Ti-based alloys [26,27] for aerospace applications. These studies have shown that hot deformation in either two-phase field or cold deformation of a β processed $\alpha + \beta$ alloy, followed by two-phase anneal led to the formation of a bimodal microstructure, consisting of primary equiaxed α, in a matrix of transformed β. Mechanistic understanding of the microstructure that develops during hot extrusion suggests that there are two operative mechanisms [27,28]. (i) Recrystallization in α plates followed by penetration into the β phase, a consequence of surface tension, i.e., driven by surface energy; (ii) dynamic globularization of the lamellar structure initiated at high local strain regions, at prior β grain boundaries. It is also known that the size of recrystallized primary α grains is related to the dimensions of the α plates that are subjected to deformation and recrystallization. The remaining high temperature β phase results in the transformed β matrix on cooling.

Extending the above principles, the Ti–Ta–Nb alloy has been subjected to a similar thermo-mechanical processing route and studied in detail, to examine the microstructure. The present study has shown that the desirable duplex microstructure has predominantly polygonal α along with small amount of acicular α and isolated β particles. The development of such a microstructure during the two stages of treatment can be understood as follows: Hot extrusion of the β annealed alloy in the two-phase field would have resulted in a bimodal structure of equiaxed primary α in a transformed β matrix as discussed above. It is reported [29] that though hcp-α' forms in both β isomorphous and eutectoid systems, the product of decomposition during tempering are different in these systems. The hexagonal α' decomposes into α phase and non-coherent intermetallic compound through several stages in the case of eutectoid systems, while in the case of isomorphous systems, α' decomposes into equilibrium α and β phases directly, where the β phase heterogeneously nucleates at the lath boundaries and internal substructures. The composition of α' approaches that of α, in equilibrium with β, depending on the temperature and duration of the treatment. Hence, the precipitation of β phase as fine, isolated, globular particles is expected to be due to tempering of the β quenched alloy as discussed in Section 3.4. From a tempered α' matrix the equiaxed α grains form by cold deformation and annealing low in the $\alpha + \beta$ phase field. Since deformation is carried out at room temperature, neither dynamic recrystallization nor diffusion of constituent elements, is expected to take place during swaging. Therefore, the process during cold swaging is mainly the break down of the acicular product, generating a high density of stress raisers and increase in the dislocation density. This leads to extensive heterogeneous sites for nucleation of α. The subsequent stress relieving treatment reduces the defect density, leading to formation of equiaxed primary α grains, whose growth is dictated by the 'hold time' during stress relieving treatment leaving behind some of the smaller β precipitates.

Based on the above discussions, it is clear that β quenching and stress relieving treatments are necessary intermediate steps in the processing sequence to obtain nodular β, while the subsequent cold deformation followed by a low temperature anneal leads to the formation of a large amount of polygonal α grains.

Hence, to obtain large volume fraction of coarse equiaxed α grains and nodular β precipitates in $\alpha + \beta$ titanium alloys, the following major guidelines could be adopted.

- obtaining coarse acicular α by cooling the alloy slowly from above the β phase field prior to deformation (initial condition after melting the alloy),
- a large hot deformation of the β processed ingot, high in the two-phase field for better workability,
- a β quenching treatment to have a fully α' structure followed by tempering treatment low in the $\alpha + \beta$ phase field, to form nodules of β,
- cold working with intermediate annealing in low temperature range in the duplex phase field, to increase the nucleation frequency during recrystallization and
- allowing sufficient time at any temperature in the $\alpha + \beta$ phase field for the growth of recrystallized α nuclei.

The simulated two-stage treatment of the TMP alloy resulted in a mixed microstructure consisting of α' and fine β nodules in a matrix of tempered martensite. This can be attributed to the tempering of the β quenched alloy high in the $\alpha + \beta$ phase field which results in the formation of coarse β phase along the grain boundary triple points and fine β precipitates on lath boundaries and internal substructures. Since the treatment is high in the two-phase field, the solute content of β phase is expected to be low. Further on quenching, while the coarse β phase along the grain boundary triple points transform to α', the fine β precipitates on lath

boundaries and internal substructures remain untransformed. Retention of these β precipitates is attributed to their fine size [21] rather than their stability acquired due to compositional difference, since they form at the same temperature.

The inability to retain the desired duplex structure in the alloy when subjected to a subsequent β treatment, as observed in the present study, warrants caution during processing of the alloy. It is therefore essential to avoid β treatments either by design or inadvertently after achieving the duplex structure.

5. Summary

This paper presented the results of an experimental study on (i) identification of a suitable microstructure in Ti–5%Ta–1.8%Nb alloy for use in high corrosive environment of boiling nitric acid and (ii) selection of a suitable thermo-mechanical processing route to achieve this microstructure. The salient features of the study are highlighted below.

- The α and β phases in Ti–5%Ta–1.8%Nb alloy assume several morphologies and distributions, of which, the distribution of β phase as random, isolated, nodular particles in a predominantly polygonal α matrix exhibits the best corrosion resistance.
- The required duplex structure, having predominantly polygonal α with small amounts of acicular α and discrete β particles could be achieved only by sequential deformation with intermediate stress relieving treatment. The equiaxed α structure could not be retained or reproduced by heat treatments if a β treatment is carried out.
- Thermal exposure of the β annealed alloy alone is not adequate to achieve the desired structure.
- The formation of β as discrete particles takes place during tempering of the martensite obtained by a β quenching treatment.
- The role of thermo-mechanical processing in achieving an equiaxed α structure has been clearly demonstrated.

Acknowledgments

The authors wish to acknowledge Dr Baldev Raj, Director, IGCAR, for giving us this opportunity to work in this exciting field and his keen interest, concern and encouragement throughout the execution of the project. The constant support provided by Dr S.L. Mannan, Director, Metallurgy and Materials Group and Dr R. Natarajan, Associate Director, Reprocessing Group also is sincerely acknowledged.

References

[1] W.E. Berry, Corrosion in Nuclear Applications – Corrosion Monograph Series, Wiley, New York, 1971, p. 23.
[2] E. Otero, A. Pardo, E. Saenb, M.V. Utrilla, P. Hierro, Corr. Sci. 38 (9) (1996) 1485.
[3] F. Balbaud, G. Sanchez, P. Fauvet, G. Santarini, G. Picard, Corr. Sci. 42 (10) (2000) 1685.
[4] K. Kiuchi, H. Hayakawa, Y. Takagi, M. Kikuchi, in: New Alloy Development for Fuel Reprocessing Plant Materials Used in Nitric Acid Solutions, A poster paper in session: 'Corrosion and Materials Selection', Proceedings of the Fourth International Conference on Nuclear Fuel Reprocessing and Waste Management, RECOD'94, London, vol. III, 24–28 April 1994.
[5] T. Motooka, K. Kiuchi, Corrosion 58 (8) (2002) 703.
[6] A. Takamura, K. Arakawa, Y. Moriguchi, in: R.I. Jaffee, N.E. Promisel (Eds.), The Science, Technology and Application of Titanium, Pergamon Press, Oxford, 1970, p. 209.
[7] C. Bernard, J.P. Mouroux, in: Proceedings of the Third International Conference on Nuclear Fuel Reprocessing and Waste Management, RECOD'91, Sendai, Japan, vol. II, 14–18 April 1991, p. 570.
[8] C.S. Brossia, G.A. Cragnolino, Corrosion 57 (9) (2001) 768.
[9] Corrosion Characteristics of Titanium in 'Corrosion Resistance of Titanium', Publication of Imperial Metal Industries, Witton, UK, 1969, p. 39.
[10] K. Kapoor, Vivekanand Kain, T. Gopalakrishna, T. Sanyal, P.K. De, J. Nucl. Mater. 322 (1) (2003) 36.
[11] S. Sundaresan, G.D. Janaki Ram, G. Madhusudhan Reddy, Mater. Sci. Eng. A 262 (1999) 88.
[12] H.M. Flower, Mater. Sci. Technol. 6 (1990) 1082.
[13] V.R. Raju, R.K. Dayal, Private Communication (2002).
[14] A. Ravi Shankar, R. Mythili, V.R. Raju, S. Saroja, R.K. Dayal, M. Vijayalakshmi, V.S. Raghunathan, R. Balasubramaniam, L.K. Singhal, in: Baldev Raj, K. Bhanu Sankara Rao, P. Shankar, N. Murali (Eds.), Proceedings of the Conference on Materials and Technologies for Nuclear Fuel Cycle, Chennai, India, 15–16 December 2003, p. C-7.
[15] F.J. Gill, M.P. Genebra, J.M. Manero, J.A. Planell, J. Alloys Compds. 329 (2001) 142.
[16] X.D. Zhang, P. Bonniwell, H.L. Fraser, W.A. Baeslack III, D.J. Evans, T. Ginter, T. Bayha, B. Cornell, Mater. Sci. Eng. A 343 (2003) 210.
[17] R. Mythili, V. Thomas Paul, S. Saroja, M. Vijayalakshmi, V.S. Raghunathan, Mater. Sci. Eng. 390A (2005) 299.
[18] N. Gey, M. Humbert, H. Moustahfid, Scr. Mater. 42 (6) (2000) 525.
[19] Metals Hand Book, vol. 7, Atlas of Microstructures of Industrial Alloys, 8th Ed., ASM, Materials Park, OH, USA, 1972, p. 321.
[20] F.J. Gill, J.M. Manero, J.A. Planell, in: P.A. Blekinshop, W.J. Evans, M. Flower (Eds.), Titanium'95: Science and Technology, Proceedings of the Eighth World Conference on Titanium, Birmingham, vol. III, 22–26 October 1995, p. 2454.
[21] I. Weichen, Y.H. Chiao, K. Tsuzaki, Acta Metall. 33 (10) (1985) 1847.

[22] R. Mythili, A. Ravi Shankar, S. Saroja, V.R. Raju, M. Vijayalakshmi, R.K. Dayal, V.S. Raghunathan, R. Balasubramaniam, communicated to J. Mater. Eng. Perform.
[23] T. Karthikeyan, Arup Dasgupta, S. Saroja, M. Vijayalakshmi, in: XXVI Annual Conference on Electron Microscopy and Allied Fields, Shimla, 16–18 April 2003, p. 197.
[24] G. Lutjering, Mater. Sci. Eng. A 263 (1999) 117.
[25] H. Margolin, P. Cohen, in: H. Kimura, O. Izumi, (Eds.), Titanium' 80: Science and Technology, Proceedings of the Fourth International Conference on Titanium, Kyoto, Japan, vol. 4, 19–22 May 1980, p. 2991.
[26] G.W. Kuhlman, in: Y.-W. Kim, R.R. Boyer (Eds.), Microstructure/Property Relationships in Titanium Aluminides and Alloys, TMS Pub., Pennsylvania, 1991, p. 465.
[27] G. Lutjering, Mater. Sci. Eng. A 243 (1998) 32.
[28] V. Seetharaman, S.L. Semiatin, I. Weiss, J. Met. June (1997) 34.
[29] J.C. Williams, in: R.I. Jaffee, H.M. Burte (Eds.), Titanium Science and Technology, vol. 3, Plenum, New York, 1973, p. 1433.